Exergy analysis of a combined heat and power plant with integrated lignocellulosic ethanol production

Lythcke-Jørgensen, Christoffer Ernst; Haglind, Fredrik; Clausen, Lasse Røngaard

Published in:
Energy Conversion and Management

Link to article, DOI:
10.1016/j.enconman.2014.01.018

Publication date:
2014

Document Version
Peer reviewed version

Exergy analysis of a combined heat and power plant with integrated lignocellulosic ethanol production

Christoffer Lythcke-Jørgensen[a]* Fredrik Haglind[b], Lasse R. Clausen[c]

[a] Technical University of Denmark, Department of Mechanical Engineering, Nils Koppels Allé 403, DK-2800 Kgs. Lyngby, celjo@mek.dtu.dk

[b] Technical University of Denmark, Department of Mechanical Engineering, Nils Koppels Allé 403, DK-2800 Kgs. Lyngby, frh@mek.dtu.dk

[c] Technical University of Denmark, Department of Mechanical Engineering, Nils Koppels Allé 403, DK-2800 Kgs. Lyngby, lrc@mek.dtu.dk

* Corresponding author. +45 30 42 72 00. Email: celjo@mek.dtu.dk.

Abstract

Lignocellulosic ethanol production is often assumed integrated in polygeneration systems because of its energy intensive nature. The objective of this study is to investigate potential irreversibilities from such integration, and what impact it has on the efficiency of the integrated ethanol production. An exergy analysis is carried out for a modeled polygeneration system in which lignocellulosic ethanol production based on hydrothermal pretreatment is integrated in an existing combined heat and power (CHP) plant. The ethanol facility is driven by steam extracted from the CHP unit when feasible, and a gas boiler is used as back-up when integration is not possible. The system was evaluated according to six operation points that alternate on the following three different operation parameters: Load in the CHP unit, integrated versus separate operation, and inclusion of district heating production in the ethanol facility. The calculated standard exergy efficiency of the ethanol facility varied from 0.564 to 0.855, of which the highest was obtained for integrated operation at

minimum CHP load and full district heating production in the ethanol facility, and the lowest for separate operation with zero district heating production in the ethanol facility. The results suggest that the efficiency of integrating lignocellulosic ethanol production in CHP plants is highly dependent on operation, and it is therefore suggested that the expected operation pattern of such polygeneration system is taken into account when evaluating the potential of the ethanol production.

Keywords

Biofuel production; exergy analysis; lignocellulosic ethanol; polygeneration; system operation

1. Introduction

The integrated production of biofuels in thermal power plants has received increasing attention in the recent years due to the potential synergies from thermal integration. One example is the gasification-based coproduction of heat, electricity, Fischer-Tropsch fuels, dimethyl ether (DME), and hydrogen from biomass feedstocks [1], like switchgrass [2] and black-liquor [3]. Another important example is the integrated production of bioethanol and synthetic natural gas (SNG) with combined heat and power (CHP) production [4]. Among biofuels, bioethanol is the most widely used for transportation on a global basis and is consumed both as an individual fuel and in blends with gasoline [5]. Bioethanol can be produced from sugars, starch, and lignocellulosic biomass, of which the latter often is considered the most sustainable option as it offers the possibility of reducing CO_2 emissions from transportation without linking fuel prices and food prices directly [4]. This study treats the integrated production of lignocellulosic ethanol in an existing CHP plant. Several studies have focused on thermal integration synergies in systems with integrated production of power, heat, lignocellulosic ethanol, and SNG [6-10]. Daianova et al. [6] and Ilic et al. [7] both report better energy economy for the integrated system compared to stand-alone systems, while Bösch et al. [8] reports a potential increase in both first law energy efficiency and exergy efficiency

when integrating the processes. Modarresi et al. [9] applied pinch analysis to improve the heat integration of the system, which yielded an integrated exergy efficiency of 88% for the ethanol process. Gassner and Maréchal [10] have investigated process integration in such polygeneration systems and conclude that both first and second law energy efficiencies are increased significantly by integrating lignocellulosic ethanol and SNG production in a CHP plant. Furthermore, a case study by Starfelt et al. [11] reports higher first-law energy efficiency for integrating lignocellulosic ethanol production in an existing CHP plant compared to a scenario with separate production. These results explain the industrial interest in retrofitting existing CHP units to obtain the mentioned polygeneration system benefits.

A previous study by the authors [12] evaluated the energy economy of integrating lignocellulosic ethanol production based on the hydrothermal pretreatment technology IBUS[1] [13] in the existing Danish CHP unit Avedøreværket 1 (AVV1). During integration, the hot utility demand of the ethanol facility was met by steam extracted from the turbines of AVV1, and when integration was not feasible due to high CHP loads or periods of CHP shut-down, a natural gas boiler was used to deliver the necessary heat while the power demand was met by power bought from the power market. The study suggested an ethanol production energy cost of 0.14 Euro/L on average during integrated operation, and 1.22 Euro/L on average during separate operation, underlining the potential benefits of integrating the production. Based on existing production patterns for AVV1, the study further suggested that the duration of separate operation over a year would be significant, reducing the overall benefit from the integration and questioning the average yearly efficiency of the ethanol production. In this study, the differences in exergy efficiency for various operation modes of the polygeneration system are investigated.

[1] IBUS (Integrated Biomass Utilization System) is a patented lignocellulosic biomass pretreatment technology. The patent is owned by the Danish company Inbicon A/S, a subsidiary to DONG Energy.

The overall objective of this study is to determine the irreversibilities related to the integration of lignocellulosic ethanol production in CHP units at various operation modes. This objective is targeted through a case study of a polygeneration system in which lignocellulosic ethanol production based on IBUS technology is integrated in the Danish CHP unit AVV1. Exergy analysis [14] is applied to a model of the ethanol production facility previously developed in Lythcke-Jørgensen et al. [12] to identify exergy flows in the ethanol production facility and its heat integration network. Exergy efficiencies are calculated for the individual process steps, and the exergy efficiency of the overall ethanol production is evaluated in six different operation points, covering both integrated and separate operation, zero and full district heating production in the ethanol facility, and various loads in the CHP unit. Based on the outcomes, the impact of polygeneration system operation on the average exergy efficiency of the ethanol production is discussed. The novelty of this paper lies in the evaluation of the average system exergy efficiency by combining exergy analysis with the performance analysis in the boundary points of the feasible operation range.

In this paper, the polygeneration system design, modelling and operation are presented in Section 2 together with the exergy analysis approach. Results of the analysis are presented in Section 3 and discussed in Section 4. Finally, a conclusion on the study is given in Section 5.

2. Methodology

2.1. Polygeneration system model

A numerical model of a polygeneration system that integrates lignocellulosic ethanol production based on IBUS technology in the Danish CHP unit AVV1 was previously developed and presented by the authors [12], and the same model is used in the present study. This section presents the system design and the modelling approach, system operation, and obtained data that are used in the

exergy analysis. A simplified process layout of the modelled polygeneration system is presented in Figure 1.

2.1.1. Modelling of AVV1

A numerical model of AVV1, developed by Elmegaard and Houbak [15] in the energy system simulator Dynamic Network Analysis (DNA) [16], was used for simulating flows and operation of AVV1. The model accuracy was evaluated at various loads by comparing electrical efficiencies, η_{el}, and first law energy efficiency, η_I, obtained in the model with efficiencies reported by the plant operator [17]. The two efficiencies are defined by the following equations:

$$\eta_{el} = \frac{P}{\dot{Q}_{fuel}} \quad (1)$$

$$\eta_I = \frac{P+\dot{Q}_{DH}}{\dot{Q}_{fuel}} \quad (2)$$

In the equations, P is the power production, $\dot{Q}_{DH}$ is the district heating production, and $\dot{Q}_{fuel}$ is the fuel input. The comparison was limited to condensation mode and full back-pressure mode operation as they represent the extreme cases of plant operation. Calculated and reported efficiencies are summarized in Table 1 and Table 2.

It was found that the model assumed slightly larger fuel consumption in condensation mode than what was reported by the plant owner, resulting in electrical efficiencies that were between 2% and 8% lower for the model. For back pressure operation, the first law energy efficiency accuracy was found to be within a range of 2%, while the electrical efficiency deviated by up to 6%. The inaccuracy of the model was found to be related to the prediction of fuel consumption mainly, and the model was therefore considered adequate for use in the present study.

2.1.2. Modelling and dimensioning of the ethanol facility

In the ethanol facility, the lignocellulosic structure of the straw is broken down through treatment with pressurized steam in the hydrothermal pretreatment stage, whereupon the straw-steam mixture

is split into a fibre fraction and a liquid fraction. The fibre fraction is liquefied by glucose-forming enzymes before fermentation is initiated in simultaneous fermentation and saccharification (SSF) tanks. Ethanol is distilled from the resulting fermentation broth, leaving a fibre stillage which is treated in various separation stages alongside the pretreatment liquid fraction, generating a solid biofuel fraction, a molasses fraction, and a waste water fraction. The molasses fraction can be used in anaerobic fermentation to produce biogas [9] or as animal feed [18], while the solid biofuel can be used for combustion or gasification.

A model of the ethanol facility based on heat and mass balances over the system process steps was developed in a previous study by the authors [12] using the software Engineering Equation Solver (EES) [19]. The model was based on the layout reported by Larsen et al. [18] and Østergaard et al. [20]. Mass balances were calculated over each process step as

$$\sum \dot{m}_{in} = \sum \dot{m}_{out} \qquad (3)$$

In flows with multiple compounds, the mass fraction of a compound i is termed x_i. The fraction of compound i recovered in a given output flow, $\varepsilon_{(flow),i}$, was defined as

$$\varepsilon_{(flow),i} = \frac{\dot{m}_{(flow)} x_{(flow),i}}{\sum_{n=inlet\ flows} \dot{m}_n x_{n,i}} \qquad (4)$$

In process steps with compound conversion or degradation, the relation of output to input mass flow of a compound i, $\eta_{(flow),i}$, was defined as

$$\eta_{(flow),i} = \frac{\sum_{k=outlet\ flows} \dot{m}_k x_{k,i}}{\sum_{n=inlet\ flows} \dot{m}_n x_{n,i}} \qquad (5)$$

The steam mass flow $\dot{m}_{steam}$ into the hydrothermal pretreatment process was modelled as a constant, K_{steam}, times the input biomass mass flow, $\dot{m}_{biomass}$, as suggested by Bentsen et al. [21].

$$\dot{m}_{steam} = K_{steam} \dot{m}_{biomass} \qquad (6)$$

To determine resulting heating or cooling demand $\dot{Q}_j$ for a process j, the energy balance over the process step was calculated as

$$\dot{Q}_j = \sum_{n=inlet\ flows} \dot{m}_n h_n - \sum_{k=outlet\ flows} \dot{m}_k h_k \quad (7)$$

Here, h_i is the specific enthalpy of the flow i. The only exception to this was the distillation process, for which the hot and cold utility demands were calculated using the Aspen Plus [22] distillation column model.

The hydrolysis of cellulose to glucose, occurring during enzymatic liquefaction and simultaneous saccharification and fermentation (SSF), follows the reaction

$$C_6H_{10}O_5 + H_2O \rightarrow C_6H_{12}O_6 \quad (8)$$

The fermentation of glucose to ethanol during SSF follows the reaction

$$C_6H_{12}O_6 \rightarrow 2 \cdot C_2H_5OH + 2 \cdot CO_2 \quad (9)$$

For both reactions, molar weight ratios were used to relate the weight fraction increase of the reaction products to the weight fraction decrease of the reactants. The parameters used in the model to describe the system are summarized in Table 3, together with parameter values reported in literature.

In the model, degradation of hemicelluloses was assumed to occur solely during pretreatment, and no degradation or dissolving of lignin was considered in the processes. Hydrolysis was assumed to be the only means of cellulose conversion. The addition of yeast and enzymes was neglected in mass balance calculations. Cellulose, hemicellulose, lignin, and glucose were assumed to have constant heat capacities in the relevant temperature ranges, and mixtures of water and ethanol with ethanol mass fractions at or below 0.1 have been treated as if the water and ethanol were separated.

The accuracy of the ethanol facility model was evaluated by comparing model yields with yields reported for IBUS-based systems by literature [13, 18, 21, 23], see Table 4.

It is seen that the yields reported by literature vary significantly. Compared to the yields reported the most recently [13], the model deviated by up to 6%. Due to the high uncertainties in facility yields reported in literature, the found accuracy was considered adequate for the present study.

The cost for biomass transportation is central when scaling facilities and developing business cases in the biorefinery sector [24]. To reflect this, a maximum wheat straw transportation distance of 50km was considered for the modelled system as suggested by the IBUS technology owner [17]. A total of 196,000 tons of winter wheat straw is cultivated within this distance from the plant [25]. The ethanol facility was dimensioned to process all locally available winter wheat, resulting in a facility processing capacity of 22.4 tons of straw per hour, or 6.22 kg/s, all year round. A linear relation between biomass processing capacity and energy consumption was used for determining the energy demand of the ethanol facility. The power consumption was set to 220kWh/ton of biomass treated as reported by Bentsen et al. [21]. Description, thermodynamic properties, and absolute mass flows of all numbered flows in the ethanol facility are given in Table 5.

2.1.3. Integration design

Based on temperature and pressure requirements for the steam to be delivered to the ethanol facility, a combined pinch analysis [26] and exergy analysis [14] was carried out to identify the best possible integration design, and the resulting steam, hot, and cold utility demands. District heating production with a forward temperature of 100°C and a return temperature of 50°C [15] was included in the pinch analysis to reduce the cooling load in the ethanol facility production. A 10K pinch temperature difference was used, as suggested by Modarresi et al. [9] for a similar facility. The exergy analysis was applied to identify the integration solution having the lowest overall exergy destruction. The results of this analysis were previously presented in Lythcke-Jørgensen et al. [12]. The optimal integration solution involved steam extraction from three steam extraction points, marked (A), (B) and (C) in Figure 1. The thermodynamic states of steam in the three points are summarized in Table 6. Steam for hydrothermal pretreatment was extracted from node (B) in AVV1 at CHP loads above 0.6, and from node (A) at CHP loads below 0.6. The steam for hydrothermal pretreatment was conditioned in the heat integration network to meet the exact

temperature and pressure requirements of the hydrothermal pretreatment component, being 195°C and 13bar [17]. Heat released from steam conditioning was used internally in the ethanol facility. The remaining hot utility demand of the ethanol facility was covered by steam extracted from node (C). Heat from the extracted steam is released in the heat integration network from where it is distributed to the facility process steps. The condensate is recycled to the condenser of AVV1 where additional desalinated water is added to compensate for the loss of steam to the hydrothermal pretreatment. Cooling in the heat integration network is provided by sea water and by district heating water when district heating production is active in the ethanol facility.

2.2. System operation

Because of load transition times of more than 180 hours in the ethanol production facility [12], the ethanol production is assumed operated at full load all year round. As the same is not the case for AVV1, the ethanol production in the polygeneration system can be run in two ways: Integrated mode or separate mode. In integrated mode, steam extracted from turbines of the CHP unit is used for covering the hot utility demand of the ethanol facility, and the power demand is met by power from the CHP unit. In separate mode, a natural gas boiler with a first law energy efficiency of 0.96 is used for generating the steam required by the ethanol facility, and the power requirement is met by power bought from the grid. Separate operation occurs during periods of high CHP unit loads where no surplus capacity for steam extraction exists, and during periods of CHP unit shut-down due to maintenance or lack of demands for heat and power production in the energy system. The two polygeneration system operation modes are outlined in Figure 2.

Pinch analysis [26] was applied to determine the hot utility demand, the internal reuse of heat, and the cooling load of the ethanol production facility. The results are presented in Lythcke-Jørgensen et al. [12]. The cooling load allowed for the production of district heating to the existing network, which is operated with a forward temperature of 100°C and a return temperature of 50°C [15]. The

pinch point for the facility was found to be 91°C, meaning that heat is readily available in the system to heat the return water from the district heating grid to this temperature at highest. As the forward temperature of the district heating grid is 100°C, additional heat is required to raise the temperature of the district heating water to the required 100°C, meaning that the hot utility demand of the ethanol facility was increased when district heating production was included. It was found that for each unit of extra heat added, 4.73 units of district heating are produced and the cold utility demand is significantly reduced. Sankey diagrams, illustrating the internal heat flows in the ethanol facility at zero and maximum district heating production, are presented in Figure 3.

This study investigates the exergy efficiency of the ethanol facility in six polygeneration system operation points with varying operation modes, CHP unit loads, and district heating production in the ethanol facility. Characteristics of the six points are given in Table 7.

2.3. Exergy analysis

Exergy analysis [14] was applied to the ethanol facility to identify irreversibilities at the different operation points. The reference point for all exergy calculations was set to $T_0 = 298.15K$ and $p_0 = 1bar$.

2.3.1. Exergy calculations

The specific exergy of a material stream, ex, was calculated as

$$ex = ex_{phys} + ex_{kin} + ex_{pot} + ex_{chem} \quad (10)$$

Here, ex_{phys} is the specific physical exergy, ex_{kin} is the specific kinetic exergy, ex_{pot} is the specific potential exergy, and ex_{chem} is the specific chemical exergy. ex_{kin} and ex_{pot} were not considered in the analysis as they are negligible in magnitude for the given material streams [8]. Exergy flows related to mass flows in the system, $\dot{EX}$, were calculated as the total specific exergy of the material stream, ex, times the mass flow of the stream, $\dot{m}$.

$$\dot{EX} = ex \cdot \dot{m} \qquad (11)$$

Considering all useful material streams out of a process as valuable, the standard exergy efficiency η_{ex} of a process step was calculated as the exergy content in product flows, $\sum \dot{EX}_{products}$, divided by the exergy content in inlet flows, $\sum \dot{EX}_{in}$.

$$\eta_{ex} = \frac{\sum \dot{EX}_{products}}{\sum \dot{EX}_{in}} \qquad (12)$$

In this study, the difference between the exergy content in inlet mass flows and in product mass flows from a process was caused partly by exergy destruction, partly by exergy content in unused heat or material flows from the process. For simplicity, these fractions were merged in a term called exergy losses and destruction (L&D), $\dot{EX}_{L\&D}$, which was calculated as

$$\dot{EX}_{L\&D} = \sum \dot{EX}_{in} - \sum \dot{EX}_{products} \qquad (13)$$

As the main products of the ethanol facility are lignocellulosic ethanol and solid biofuel for combustion, the fuel exergy efficiency, $\eta_{ex,fuel}$, was evaluated for the ethanol facility as well.

$$\eta_{ex,fuel} = \frac{\dot{EX}_{ethanol} + \dot{EX}_{solid\ fuel}}{\sum \dot{EX}_{in,system}} \qquad (14)$$

2.3.2. Chemical exergy

The chemical exergy of multi-component material streams, ex_{chem}, was calculated as the sum of the chemical exergy content of the individual process steps $ex_{chem,i}$ multiplied by their weight fraction x_i:

$$ex_{chem} = \sum_i ex_{chem,i} x_i \qquad (15)$$

The chemical exergy of materials that are found in the ethanol facility is summarized in Table 8. As suggested by Rian et Ertesvåg [27], the chemical exergy of natural gas was set to 43,497 kJ/kg and the lower heating value to 41,426 kJ/kg.

2.3.3. Physical exergy

As material flows in the system occur at reference pressure, the mechanical part of the physical exergy is zero. As suggested by Bösch et al. [8], heat capacities of biomass material streams were assumed constant over the relevant temperature ranges. The physical exergy of multi-component biomass materials was calculated according to the specific heat capacity of the material, c_p, and the temperature of the material, T, using the following equation [14].

$$ex_{phys,biomass} = c_p \left(T - T_0 - \ln\left(\frac{T}{T_0}\right)\right) \quad (16)$$

The heat capacity of multi-component materials was calculated as the sum of heat capacities of the individual process steps, $c_{p,i}$, multiplied by their weight fraction x_i. The values used are presented in Table 8.

$$c_p = \sum_i c_{p,i} x_i \quad (17)$$

2.3.4. Exergy in heat flows

The exergy content of heat flows in the system is associated with the exergy content in the heat exchange media used. In the ethanol facility, water was assumed used as heat exchange media. As mentioned, heat is provided in the form of steam from the CHP unit or a gas boiler, and cooling is provided by district heating water and sea water at the given location.

In this study, best-case heat transfer is defined as heat transfer where the temperature difference between the hot and cold streams is equal to the minimum value throughout the heat exchanger. The minimum value was set to 10K as suggested for a similar system by Modarresi et al. [9]. All losses associated with non-best-case heat exchange in the system are merged in the heat integration network in the analysis.

The reference pressure of the heat exchange media was set to 1bar, but for phase change heat exchange, the pressure is changed to maintain the 10K temperature difference over the entire phase

change of the hot and cold flows. The heat flow transferred, $\dot{Q}$, the temperature interval, the necessary mass flow, $\dot{m}$, and heat exchange media pressure, p, of all heat exchange processes in the system are presented in Table 9. Pumping in the heat integration network was not considered. Further details about heat flows and pinch analysis of the integrated system are given in Lythcke-Jørgensen et al. [12].

3. Exergy analysis results

3.1. Ethanol production

Using the method described previously, exergy flows in the ethanol facility were calculated. The results are presented in a Grassmann diagram in Figure 4. The diagram shows how the exergy content of the inlet wheat straw passes through the various processes in the facility until it ends up in the final energy products: ethanol, solid fuel and molasses. The exergy flows of heat transferred into the system, and of the heat recovered from the different process steps, all represent best-case heat exchange, as described in Section 2.3.4. The heat recovered is sent back into the heat integration network where it is reused internally, used for district heating production, or is cooled off. Exergy losses and destruction (L&D), which cover exergy destruction in process steps and exergy content of discarded material streams and heat losses, are illustrated as well. Exergy destruction in the ethanol facility is in general related to heat transfer over a temperature difference, frictional exergy destruction, heat losses, and material degradation.

The largest exergy L&D in the ethanol production was found to occur in the Simultaneous Saccharification and Fermentation (SSF) process where the exothermal fermentation process takes place. Heat released from the fermentation is used to maintain an elevated temperature in the process, and the heat released is not recovered. L&D in this process step are associated with heat losses and product degradation from the fermentation process. The exergy L&D during the

separation stage are also significant, mainly caused by large amounts of heat transfer and mechanical separation of flows. Standard exergy efficiencies of the individual process steps and the ethanol production as a whole are presented in Table 10.

The SSF is seen to be the least efficient ethanol facility process step in terms of exergy efficiency, while the ethanol production as a whole reaches a best-case exergy efficiency of 0.91.

3.2. Heat integration network and system efficiencies

Exergy flows in the heat integration network were studied for the six operation points described in Table 7. The exergy flows into and out of the heat integration network and the exergy L&D in the various operation points are summarized in Table 11. Exergy L&D in the heat integration network are related to exergy destruction from heat transfer over a temperature difference, and heat losses. Pumping work and frictional losses were not considered.

The main outcome of the results presented in Table 11 is the demonstration that exergy efficiency of the heat integration network is heavily influenced by the operation of the polygeneration system. Thus, district heating production and the choice between integrated and separate mode operation are seen to have significant impact on the exergy efficiency. Exergy efficiency is increased with district heating production as the production converts otherwise discarded heat flows, and their exergy contents, to the useful energy commodity district heating. However, this increase comes at the cost of slightly higher exergy flows into the heat integration network. Separate operation is found to decrease the exergy efficiency markedly when compared to integrated operation due to the fact that the heating source is switched from steam with low exergy-to-energy ratios to natural gas with very high exergy-to-energy ratio. The results further indicate that the exergy efficiency of the heat integration network depends only slightly on the load in the CHP unit.

For each of the six operation points of interest, the standard exergy efficiency, as defined in equation (12), and the fuel exergy efficiency, as defined in equation (14), were calculated for the entire ethanol facility. The results are presented in Table 12.

With regards to standard exergy efficiency, the ethanol facility was found to have an efficiency pattern equal to that of the heat integration network. The highest standard exergy efficiency of 0.855 was obtained in operation point IV where the production was carried out in integrated mode, the CHP unit was operated at a load of 0.4, and the district heating production in the ethanol facility was at full load. This number is quite similar to an exergy efficiency of 0.88 reported by Modarresi et al. [9] for a similar production. The lowest standard exergy efficiency of 0.564 occurred in operation point V where the ethanol facility is operated separately and no district heating production is included. Integrated operation at 0.4 partial load was found to yield higher exergy efficiencies than integrated operation at full load due to the fact that the exergy-to-energy ratio in the extracted steam was lower for the part-load operation. Grassmann diagrams of the polygeneration system in these two points are presented in Figure 5.

At variance with these results, the fuel exergy efficiency was found to be inversely proportional to the district heating production. This is due to the fact that district heating production leads to a higher heating load on the system without yielding more fuel products. The highest fuel exergy efficiency obtained was 0.795 and occurred in operation point III, while the lowest obtained was 0.520 and occurred in operation point VI.

In general, the main message obtained from the results of this study is the fact that operation can have a major impact on the efficiency of lignocellulosic ethanol production when integrated in a CHP unit. For the six operation points evaluated, the standard exergy efficiency was found to vary from 0.564 to 0.855, and operation should therefore be taken into account when estimating the actual potentials of integrating lignocellulosic ethanol with combined heat and power production. A

suggestion for further work would be to determine the average exergy efficiency of the treated ethanol facility through simulations of the yearly production for the entire polygeneration system.

4. Discussion

The results of this study suggest that operation can affect the efficiency of producing ethanol in integration with CHP plants. Three operation parameters were investigated in this study: CHP unit load, integrated versus separate operation and district heating production in the ethanol facility.

It was indicated that the CHP unit load only had a minor impact on the standard exergy efficiency of the ethanol production. The exergy content of the steam extracted was slightly lower for a load of 0.4 than for a load of 1.0 due to variations in the thermodynamic state of the steam extracted from the CHP unit at the various loads. However, this parameter was found to be the least significant of the three that were investigated.

Of the investigated parameters, separate operation was found to have the most significant negative impact on the standard exergy efficiency of the ethanol facility. Separate operation can be caused by high power loads on the CHP unit, or by periods of CHP unit shut-down. Another study of the investigated polygeneration system suggested that the separate operation would occur for almost 39% of the year in the present Danish energy system [12], and with further integration of wind power in the Danish grid it is likely that the periods of CHP shut-down will be extended in the future [28]. This might cause the average standard exergy efficiency of the ethanol production to be well below the levels calculated for integrated operation.

District heating production was found to increase the standard exergy efficiency of the ethanol facility. However, district heating is associated with both daily, weekly, and seasonally demand fluctuations. It is therefore unlikely that the benefits of district heating production can be obtained all year round.

Regarding exergy L&D in the ethanol facility, it was found that L&D in the heat integration network accounted for 45% of the total exergy losses in the best-case operation point, IV, while they accounted for 86% of the losses in the worst-case operation point, V. This suggests that the main focus point for increasing the efficiency of the system lies in the heat integration network. During integrated operation, the efficiency of the heat integration network could be increased by extracting steam with a lower exergy content that still satisfies the requirements of the ethanol production. However, a previous study [12] showed that no existing steam extraction points in the treated CHP unit could achieve this. During separate operation, the most straight forward improvement would be to replace the natural gas with another fuel or heat source that has a lower exergy-to-energy ratio. This could significantly improve the standard exergy efficiency of the ethanol facility during separate operation. Finally, the exergy efficiency of the heat integration network could be increased by technological developments of the ethanol production that will allow for a larger amount of internal reuse of heat, reducing both the hot and cold utility demands for the ethanol facility and thereby reducing the exergy losses and destruction in the heat integration network. Whether or not this is feasible is beyond the scope of this paper.

Several other research groups have investigated energy and exergy flows in systems producing lignocellulosic ethanol, heat, and power. As mentioned, Modarresi et al. [9] reported a lignocellulosic ethanol production exergy efficiency of 0.88 for a similar system, which is comparable to the 0.855 found in this study. Furthermore, the group reported a practical heat load reduction of 0.41 and a cooling load reduction of 0.40 through the application of pinch analysis, while it was only possible to reduce the heat and cooling load by 0.09 for the system investigated in this study when district heating was not included [12]. The main reason for this is the rigid choice of processing technology, and it is likely that technological changes can improve the heat integration potential significantly. This would be relevant to investigate in a future study. It should

be highlighted that the inclusion of district heating production in the ethanol production was found to reduce the cooling load by up to 0.92 [12]. Furthermore, integration synergies could be expanded by using the lignin fuel from the ethanol production in the CHP unit directly as pointed out by Starfelt et al. [11]. This was not considered in the present study.

For a comparable polygeneration system, Bösch et al. [8] reported an exergy efficiency for the ethanol production of 0.74. In the system studied, the C5-molasses from the lignocellulosic ethanol production were used for biogas production through anaerobic fermentation. The produced biogas was fed to a combustion engine for the production of electricity and a part of the heat required by the ethanol production, while the rest of the heat demand was met by a gas combustion chamber. The conversion of C5-molasses and the combustion of the produced gas seems to be the reason for the lower exergy efficiency of this system.

Due to the potential operation impact on the system efficiency, it is relevant to investigate the expected operation patterns of such polygeneration system. A previous study by the authors [12] evaluated the operation of the system by applying a historical operation pattern for the CHP unit. With this operation pattern, separate operation would occur for 3375 hours of the year, of which 2060 hours were caused by shut-down of the CHP unit and the remaining 1685 hours were caused by high heat and power loads on the CHP unit which prevented integrated operation. However, the study also suggested that the ethanol production economy is much better during integrated operation. It is therefore likely that the operation pattern of the polygeneration system would be changed to favor this production, which could be done by extending the operation time of the CHP unit over the year, and by reducing the power production of the CHP unit during peak load periods. Whether this would be done depends on a payoff between lost incomes from power sales and decreased costs for the ethanol production.

5. Conclusion

This study contained an exergy analysis of a polygeneration system in which hydrothermal pretreatment-based lignocellulosic ethanol production is integrated in the Danish combined heat and power unit Avedøreværket 1. The analysis was conducted for six different operation points that alters on three different operation parameters: Load in the CHP unit, integrated versus separate operation, and the inclusion of district heating production in the ethanol facility. The analysis suggested that the load in the CHP unit only had a minor impact on the standard exergy efficiency of the ethanol facility during integrated operation. Opposed to this, separate operation was found to yield significantly lower standard exergy efficiencies for the ethanol facility than integrated operation did. The inclusion of district heating production in the ethanol facility was found to increase the standard exergy efficiency slightly. The calculated standard exergy efficiency of the ethanol facility varied from 0.564 to 0.855, of which the highest was obtained for integrated operation at minimum CHP load and full district heating production in the ethanol facility, and the lowest for separate operation with zero district heating production in the ethanol facility. The results suggest that the efficiency of integrating lignocellulosic ethanol production in CHP plants is highly dependent on operation, and it is therefore suggested that the expected operation pattern of such polygeneration system is taken into account when evaluating the potential performance of the polygeneration system.

Acknowledgements

The authors would like to thank Brian Elmegaard for allowing the use of his numerical model of the Danish combined heat and power unit Avedøreværket 1 in the study, and for his feedback on the method used for analysing exergy flows in the system.

References

[1] J. Ahrenfeldt, T. Thomsen, U. Henriksen and L. R. Clausen, “Biomass gasification cogeneration - A review of state of the art technology and near future perspectives,” *Applied Thermal Engineering,* no. 50, pp. 1407-1417, 2013.

[2] E. D. Larson, H. Jin and F. E. Celik, “Large-scale gasification-based coproduction of fuels and electricity from switchgrass,” *Biofuels, bioproducts and biorefining,* no. 3, pp. 174-194, 2009.

[3] M. Naqvi, J. Yan and E. Dahlquist, “Black liquor gasification integrated in pulp and paper mills: A critical review,” *Bioresource Technology,* no. 101, pp. 8001-8015, 2010.

[4] M. Gassner and F. Maréchal, “Increasing Efficiency of Fuel Ethanol Production from Lignocellulosic Biomass by Process Integration,” *Energy Fuels,* no. 27, pp. 2107-2115, 2013.

[5] M. Balat, “Production of bioethanol from materials via the biochemical pathway: A review,” *Energy Conversion and Management,* no. 52, pp. 858-875, 2010.

[6] L. Daianova, E. Dotzauer, E. Thorin and J. Yan, “Evaluation of a regional bioenergy system with local production of biofuel for transportation, integrated with a CHP plant,” *Applied Energy,* no. 92, pp. 739-749, 2011.

[7] D. D. Ilic, E. Dotzauer and L. Trygg, “District heating and ethanol production through polygeneration in Stockholm,” *Applied Energy,* no. 91, pp. 214-221, 2011.

[8] P. Bösch, A. Modarresi and A. Friedl, “Comparison of combined ethanol and biogas polygeneration facilities using exergy analysis,” *Applied Thermal Engineering,* no. 37, pp. 19-29, 2012.

[9] A. Modarresi, P. Kravanja and A. Friedl, “Pinch and exergy analysis of lignocellulosic ethanol, biomethane, heat and power production from straw,” *Applied Thermal Engineering,* no. 43, pp. 20-28, 2012.

[10] M. Gassner and F. Maréchal, “Increasing Conversion Efficiency in Fuel Ethanol Production from Lignocellulosic Biomass by Polygeneration – and a Paradoxon between Energy and Exergy in Process Integration,” in *ECOS 2010*, 2010.

[11] F. Starfelt, E. Thorin, E. Dotzauer and J. Yan, “Performance evaluation of adding ethanol production into an existing combined heat and power plant,” *Bioresource Technology,* no. 101, pp. 613-618, 2009.

[12] C. Lythcke-Jørgensen, F. Haglind and L. R. Clausen, “Thermodynamic and economic analysis of integrating lignocellulosic bioethanol production in a Danish combined heat and power plant,” in *21st European Biomass Conference & Exhibition*, Copenhagen, 2013, June.

[13] J. Larsen, M. Østergaard Haven and L. Thirup, “Inbicon makes lignocellulosic ethanol a commercial

reality," *Biomass and Bioenergy,* no. 46, pp. 36-45, 2012.

[14] A. Bejan, G. Tsatsaronis and M. Moran, Thermal Design & Optimization, John Wiley & Sons, Inc., 1996.

[15] B. Elmegaard and N. Houbak, "Simulation of the Avedøreværket Unit 1 cogeneration plant with DNA," in *ECOS 2003*, Copenhagen, 2003.

[16] B. Elmegaard and N. Houbak, "DNA - A General Energy System Simulation Tool," in *SIMS*, 2005.

[17] C. Lythcke-Jørgensen, "Modelling and Optimization of a Steam Co-generation Plant with Integrated Bio-ethanol Production," Technical University of Denmark, Kgs. Lyngby, 2012. http://orbit.dtu.dk/en/projects/modelling-and-optimisation-of-novel-polygeneration-plants(3c273dec-db89-4628-839b-078cb414c573).html

[18] J. Larsen, M. Ø. Petersen, L. Thirup, H. W. Li and F. K. Iversen, "The IBUS Process - Lignocellulosic Bioethanol Close to a Commercial Reality," *Chemical Engineering & Technology,* no. 5, pp. 765-772, 2008.

[19] "F-Chart Software," [Online]. Available: http://www.fchart.com/ees/. [Accessed 25 February 2013].

[20] M. Østergaard Petersen, J. Larsen and M. Hedegaard Thomsen, "Optimization of hydrothermal pretreatment of wheat straw for production of bioethanol at low water consumption without addition of chemicals," *Biomass and Bioenergy,* no. 33, pp. 834-840, 2009.

[21] N. S. Bentsen, C. Felby and K. H. Ipsen, "Energy Balance of 2nd Generation Bioethanol Production in Denmark," Elsam A/S, 2006.

[22] AspenTech, [Online]. Available: http://www.aspentech.com/products/aspen-plus.aspx. [Accessed 16 August 2013].

[23] Inbicon A/S, "Making Ethanol Work for the World," Fredericia, Denmark, 2010. http://www.inbicon.com/sitecollectiondocuments/pdf/kacelle/kacelle_brochure.pdf

[24] M. W. Jack, "Scaling laws and technology development strategies for biorefineries and bioenergy plants.," *Bioresource Technology,* no. 100, pp. 6324-6330, 2009.

[25] Danmarks Statistik, "Statistikbanken," 2012. [Online]. Available: www.statistikbanken.dk. [Accessed 17 May 2012].

[26] I. C. Kemp, Pinch Analysis and Process Integration, 2nd edition, Oxford, UK: Butterworth-Heinemann, 2006.

[27] A. B. Rian and I. S. Ertesvåg, "Exergy Evaluation of the Arctic Snøhvit Liquefied Natural Gas Processing Plant in Northern Norway - Significance of Ambient Temperature," *Energy&Fuels,* no. 26, pp. 1259-

1267, 2012.

[28] H. Lund, B. V. Mathiesen, P. Christensen and J. H. Schmidt, “Energy system analysis of marginal electricity supply in consequential LCA,” *International Journal of Life Cycle Assessment,* no. 15, pp. 260-271, 2010.

Table 1

Table 1 - Comparison of model and reported plant efficiencies in AVV1 at condensation operation.

Condensation Mode Operation			
Load	η_{el}, model	η_{el}, reported [17]	η_{el}, deviation
1.0	0.41	0.42	-2%
0.8	0.40	0.42	-5%
0.6	0.39	0.42	-7%
0.4	0.37	0.40	-8%

Table 2

Table 2 - Comparison of model and reported plant efficiencies in AVV1 at full back pressure operation.

Full Back Pressure Mode Operation						
Load	η_{el}, model	η_{el}, reported [17]	η_{el}, deviation	η_{I}, model	η_{I}, reported [17]	η_{I}, deviation
1.0	0.36	0.34	6%	0.91	0.92	-1%
0.8	0.35	0.34	3%	0.91	0.92	-1%
0.6	0.33	0.33	0%	0.90	0.91	-1%
0.4	0.30	0.30	0%	0.88	0.90	-2%

Table 3

Table 3 - Parameters and parameter values used in the model of the IBUS facility.

	Parameter	Literature Values	Used Value
Biomass composition	Cellulose mass fraction	0.327 [18]	0.327
	Hemicellulose mass fraction	0.358 [18]	0.358
	Lignin mass fraction	0.155 [18]	0.155
	Water mass fraction	0.04 [18]	0.04
	'Others' mass fraction	0.12 [18]	0.12
Pretreatment	Steam to biomass ratio	1.93 [21][a] 2.0-2.7 [23][b]	2.0
	Cellulose recovered in fibre fraction	0.955 [18] 0.969 [21]	0.96
	Hemicelluloses recovered in the fibres	0.313 [18]	0.313
	Lignin recovered in the fibres	-	1.00
	Total hemicellulose recovery	0.68 [18]	0.68
	Water mass fraction in fibre fraction	0.7-0.75 [18] 0.6-0.75 [23]	0.35
Liquefaction	Unreacted input cellulose	0.6-0.7 [18]	0.65
	Liquefaction residence time	6h [18]	6h
Simultaneous Saccharification and Fermentation	Unreacted input cellulose	0.3-0.6[C] [18] 0.23-0.31 [21]	0.3
	SSF residence time	170h [18] 140h [23]	140h
Distillation	Ethanol in distillation product	0.93-0.95 [18]	0.95
	Ethanol in distillation stillage	0.0008 [18]	0.0008
Separation	Wet-fuel water content	0.6 [18] 0.65-0.7 [23] [d]	0.4[e]
	Dry-fuel water content	0.05-0.2 [18] 0.09 [21] 0.1 [23]	0.1
	Molasses water content	0.35 [23]	0.65
	Hemicelluloses in wet-fuel	-	0.78

[a] Equals 3.8 GJ steam/ton of straw treated

[b] Equalling operation at dry-matter contents of 30-40% in the pretreatment stage

[c] Gives an ethanol concentration of the broth in the range 0.06-0.085

[d] When using decanter technology

[e] Is assumed achievable when using a filter press instead of decanters for wet-fuel extraction

Table 4

Table 4 - Comparison of model yields and yields reported in the literature. All numbers are given in kg/ton of biomass treated.

	Model yield	[13]	[18]	[21]	[23]
Bioethanol	150.0	144	143	153.3	143.3
Solid biofuel	406.8	435	353	-	433.3
Molasses	371.0	371	420	-	370.0

Table 5

Table 5 – Descriptions and characteristics of flows in the ethanol facility. Note that the pretreatment liquid fraction (stream 7) has a lower temperature than the pretreatment fibre fraction (stream 2) as it is used to preheat the inlet straw in the pretreatment stage

Flow No.	Description	Mass flow [kg/s]	Temperature [°C]	Pressure [bar]
(1)	Inlet straw	6.22	25	1
(2)	Pretreatment fibre fraction	9.77	100	1
(3)	Liquefied fibre fraction	9.77	50	1
(4)	Fermentation broth	8.89	33	1
(5)	Ethanol	0.93	25	1
(6)	Fibre stillage	7.96	100	1
(7)	Pretreatment liquid fraction	8.89	80	1
(8)	Solid biofuel	2.53	25	1
(9)	C5-rich molasses	2.31	25	1
(10)	Steam for pretreatment	12.44	195	13
(11)	Waste water fraction	12.01	25	1
(12)	CO2 from fermentation	0.88	33	1

Table 6

Table 6 – Thermodynamic state ranges in the steam extraction points of AVV1.

Point	Temperature range [°C]	Saturation temperature range [°C]	Pressure range
(A)	431-467	199.8-241.2	15.5-34.2
(B)	359-392	176.7-213.6	9.3-20.5
(C)	257-289	145.4-176.1	4.2-9.2

Table 7

Table 7 – Characteristics of the six polygeneration system operation points investigated in the study.

Operation point no.	Integrated mode operation	Load in AVV1 [-]	District heating load [-]
I	Yes	1.0	0.0
II	Yes	1.0	1.0
III	Yes	0.4	0.0
IV	Yes	0.4	1.0
V	No	-	0.0
VI	no	-	1.0

Table 8

Table 8 – Chemical properties of material components in the ethanol facility. Heat capacities for water and ethanol are taken from the software EES [19], *chemical exergy of natural gas is taken from a study by Rian and Ertesvåg* [27], *and all other values are from a study by Bösch et al.* [8].

Material component	c_p [kJ/kg-K]	ex_{chem} [kJ/kg]
Cellulose	1.28	18,808
Hemicellulose	1.28	18,808
Lignin	1.29	25,648
Monomers	1.15	16,687
Proteins	1.30	24,488
Ash	0.70	1,006
Glucose	1.15	16,687
Ethanol	2.53	29,532
Water	4.18	51
Natural gas	-	43,497

Table 9

Table 9 – Best-case hot and cold streams in the ethanol facility during production.

Component	Flow type	$\dot{Q}$ [MJ/s]	T_{in} [C]	T_{out} [C]	p [bar]	$\dot{m}$ [kg/s]
Pretreatment	Hot	34.0	195	-	13	12.44
	Cold	2.1	90	180	0.7018	11.88
	Cold	26.7	90	91	0.7018	11.69
	Cold	0.6	70	90	1	6.78
	Cold	1.5	40	90	1	10.95
	Cold	0.4	25	40	1	5.97
Distillation	Hot	10.1	111	110	1.431	4.54
	Hot	0.1	47	43	1	7.84
	Cold	6.5	68	69	0.286	2.80
	Cold	0.2	25	90	1	0.62
Separation	Hot	27.2	111	110	1.431	12.19
	Hot	0.6	110	90	1.431	7.34
	Cold	27.2	90	91	0.7018	11.88
	Cold	5.0	25	90	1	18.47
District heating[a]	Cold	0.0 - 81.3	50	100	20	0.0 - 388.1

[a] District heating production in the ethanol facility can be varied.

Table 10

Table 10 – Standard exergy efficiency of the ethanol facility components and the overall ethanol production.

Component	Standard exergy efficiency, η_{ex}
Pretreatment	0.99
Liquefaction	0.99
SSF	0.94
Distillation	0.99
Separation	0.95
Ethanol facility, total	0.91

Table 11

Table 11 – Exergy flows into and out of the heat integration network, and its standard exergy efficiency.

	I	II	III	IV	V	VI
Exergy in steam from AVV1 extraction point A [MW]	-	-	14.2	14.2	-	-
Exergy in steam from AVV1 extraction point B [MW]	13.9	13.9	-	-	-	-
Exergy in steam from AVV1 extraction Point C [MW]	10.5	15.5	8.9	13.3	-	-
Exergy in natural gas supply [MW]	-	-	-	-	76.1	91.7
Exergy supplied to district heating [MW]	-	11.6	-	11.6	-	11.6
Exergy L&D [MW]	16.9	10.4	16.0	8.8	68.8	72.8
Standard exergy efficiency of the heat integration network [-]	0.53	0.75	0.55	0.78	0.22	0.30

Table 12

Table 12 – Standard exergy efficiency and fuel exergy efficiency for the integrated ethanol facility in the six investigated operation points.

Operation point	Standard exergy efficiency, η_{ex} [-]	Fuel exergy efficiency, $\eta_{ex,fuels}$ [-]
I	0.787	0.787
II	0.843	0.758
III	0.795	0.795
IV	0.855	0.769
V	0.564	0.564
VI	0.589	0.520

Figure 1

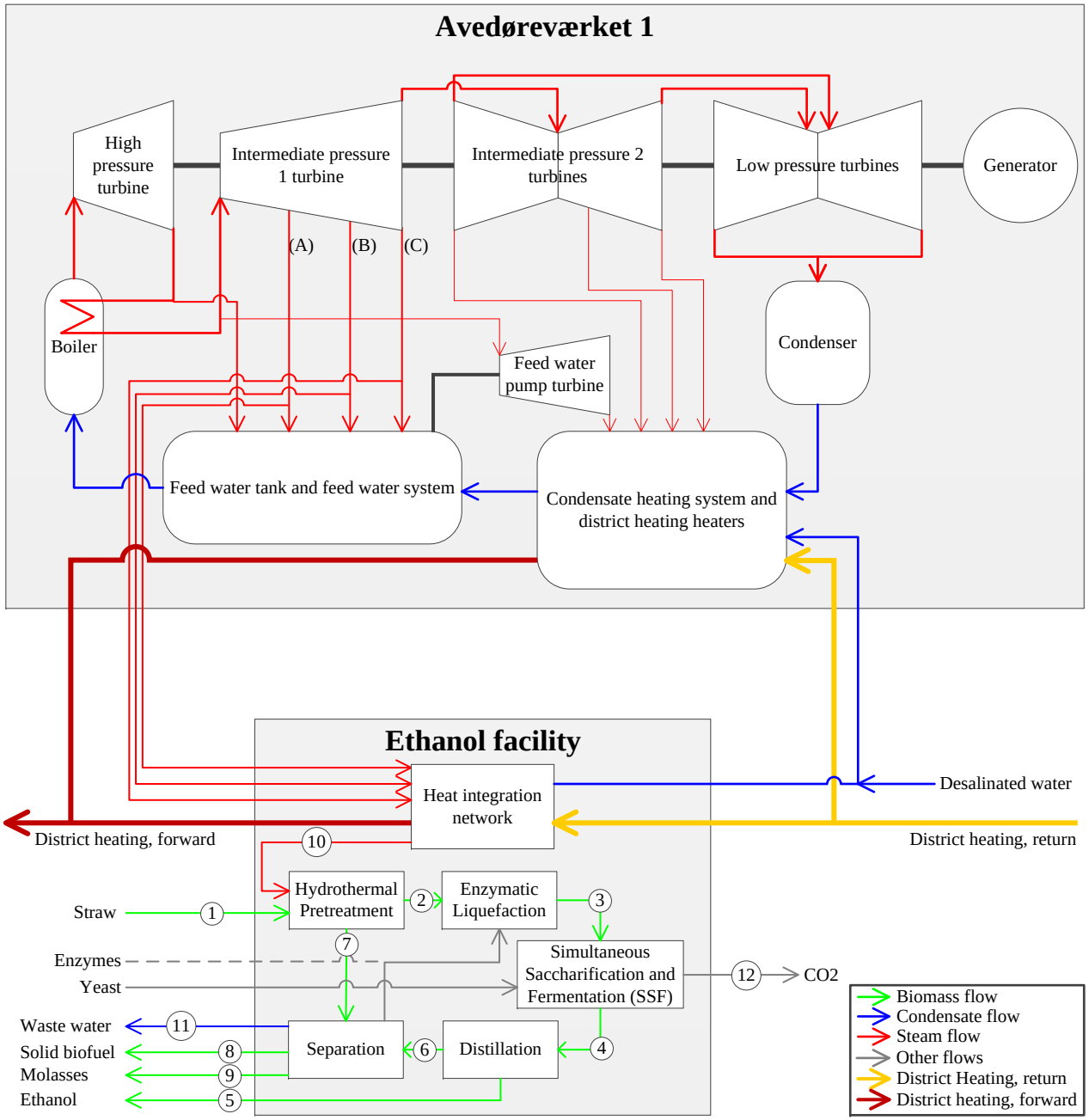
Avedøreværket 1
High pressure turbine
Intermediate pressure 1 turbine
Intermediate pressure 2 turbines
Low pressure turbines
Generator
(A)
(B)
(C)
Boiler
Feed water pump turbine
Condenser
Feed water tank and feed water system
Condensate heating system and district heating heaters
Ethanol facility
Heat integration network
Desalinated water
District heating, forward
District heating, return
10
Hydrothermal Pretreatment
2
Enzymatic Liquefaction
3
Straw
1
7
Enzymes
Yeast
Simultaneous Saccharification and Fermentation (SSF)
12
CO2
Waste water
11
Solid biofuel
8
Molasses
9
Ethanol
5
Separation
6
Distillation
4
Biomass flow
Condensate flow
Steam flow
Other flows
District Heating, return
District heating, forward

Figure 1 - caption

Figure 1 – Simplified component layout of the polygeneration system. Numbered streams are described in detail in Table 5.

Figure 2

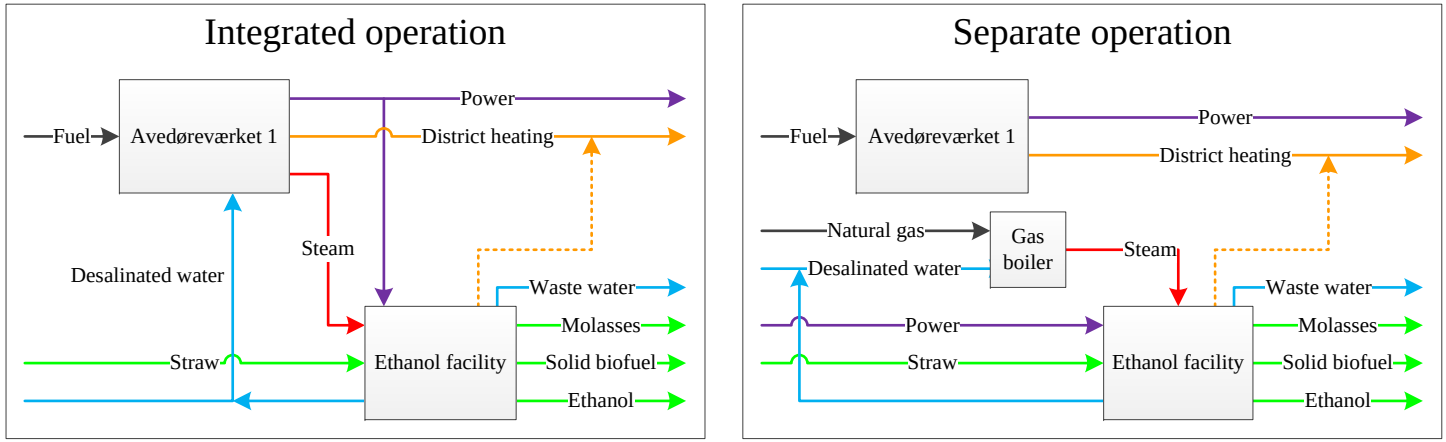
Integrated operation
Fuel
Avedøreværket 1
Power
District heating
Steam
Desalinated water
Waste water
Molasses
Straw
Ethanol facility
Solid biofuel
Ethanol
Separate operation
Fuel
Avedøreværket 1
Power
District heating
Natural gas
Gas boiler
Steam
Desalinated water
Waste water
Power
Molasses
Straw
Ethanol facility
Solid biofuel
Ethanol

Figure 2 - caption

Figure 2 – Outlines of the two operation modes in the polygeneration system.

Figure 3

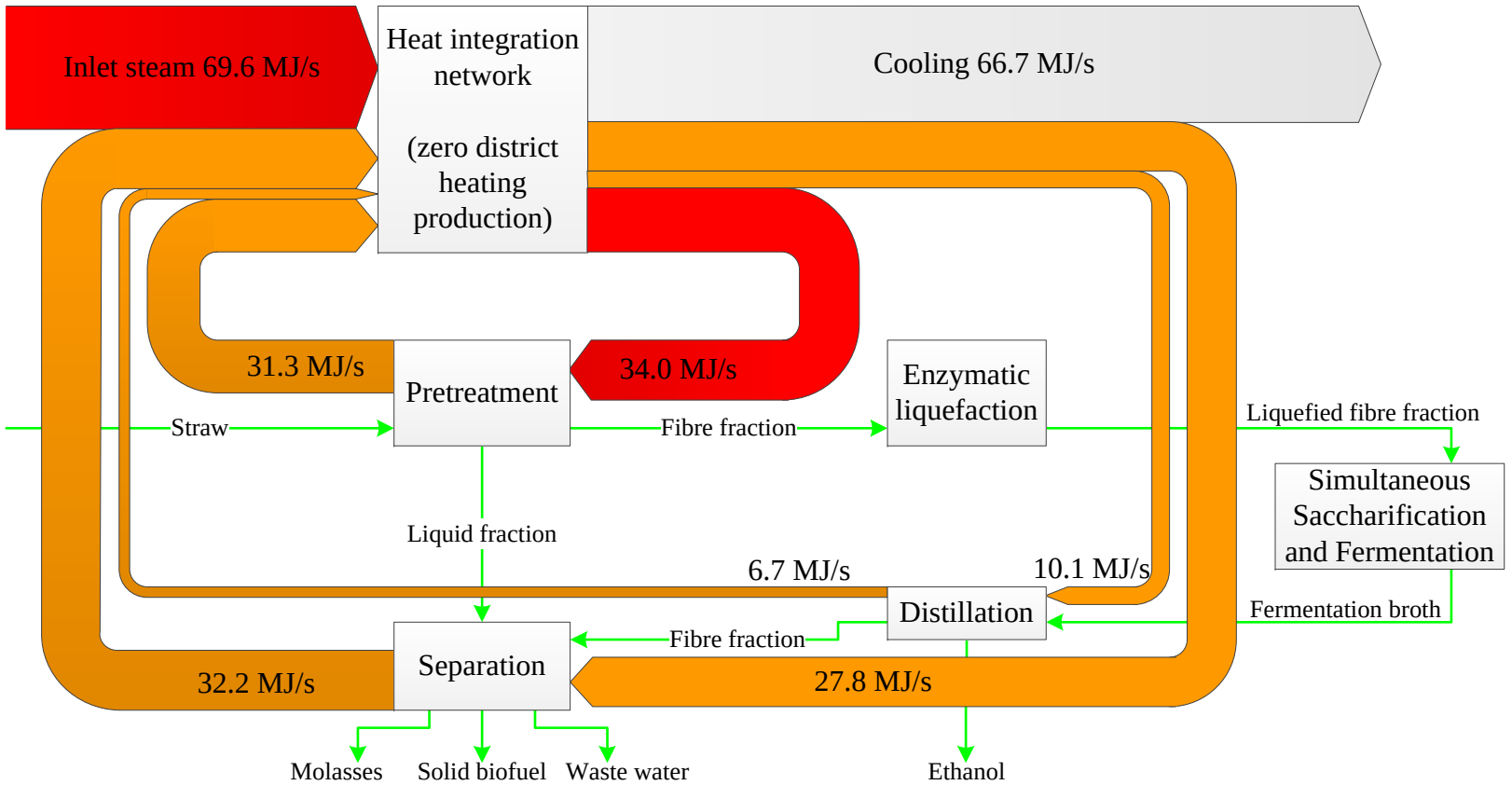
Inlet steam 69.6 MJ/s
Heat integration network
(zero district heating production)
Cooling 66.7 MJ/s
31.3 MJ/s
Pretreatment
34.0 MJ/s
Enzymatic liquefaction
Straw
Fibre fraction
Liquefied fibre fraction
Simultaneous Saccharification and Fermentation
Liquid fraction
6.7 MJ/s
10.1 MJ/s
Distillation
Fermentation broth
Fibre fraction
Separation
32.2 MJ/s
27.8 MJ/s
Molasses
Solid biofuel
Waste water
Ethanol

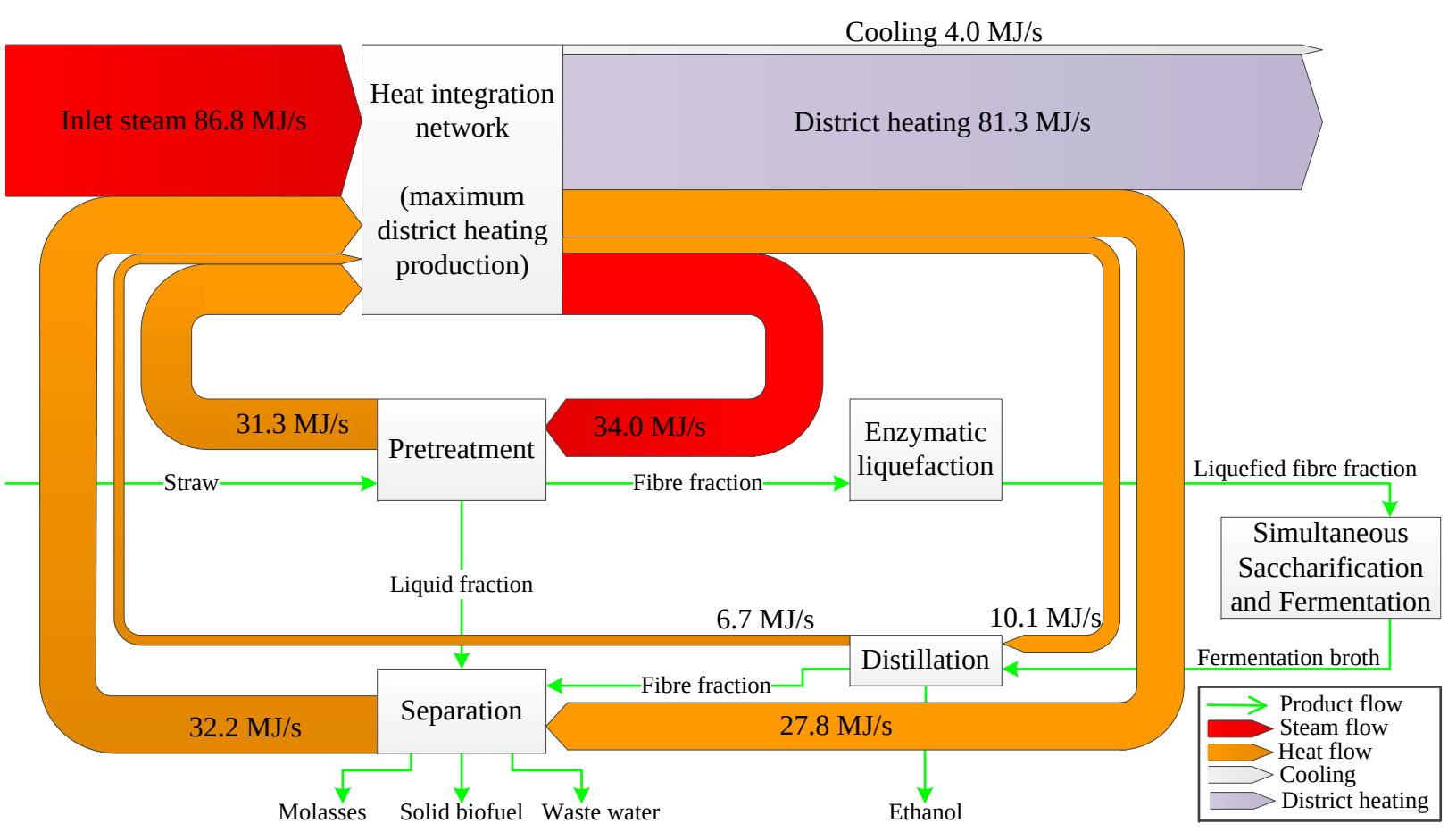
Cooling 4.0 MJ/s
Inlet steam 86.8 MJ/s
Heat integration network
(maximum district heating production)
District heating 81.3 MJ/s
31.3 MJ/s
Pretreatment
34.0 MJ/s
Enzymatic liquefaction
Straw
Fibre fraction
Liquefied fibre fraction
Simultaneous Saccharification and Fermentation
Liquid fraction
6.7 MJ/s
10.1 MJ/s
Distillation
Fermentation broth
Fibre fraction
Separation
32.2 MJ/s
27.8 MJ/s
Molasses
Solid biofuel
Waste water
Ethanol
Product flow
Steam flow
Heat flow
Cooling
District heating

Figure 3 - caption

Figure 3 – Sankey diagrams of heat flows in the ethanol facility at zero (top) and maximum (bottom) district heating production.

Figure 4

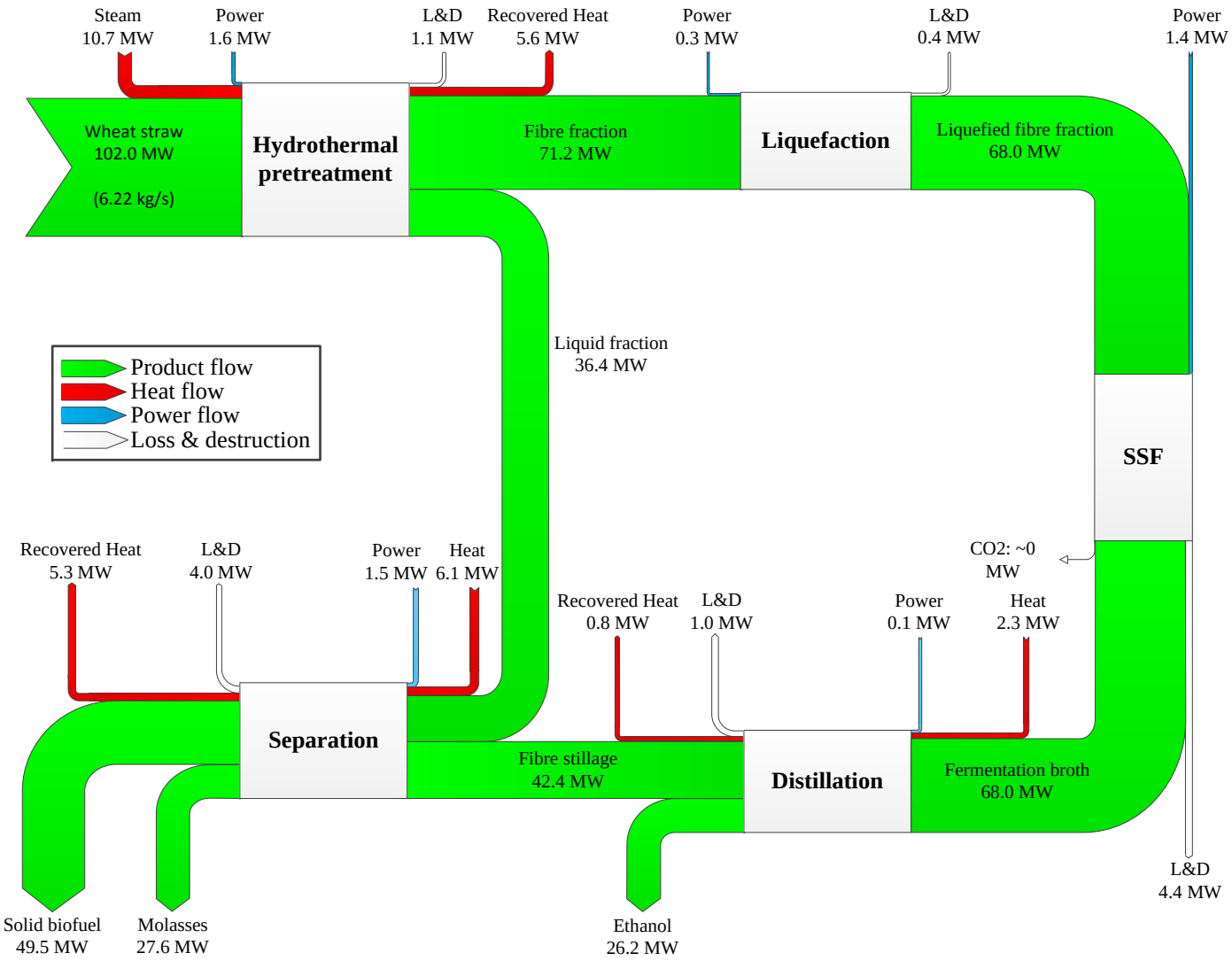
Steam
10.7 MW
Power
1.6 MW
L&D
1.1 MW
Recovered Heat
5.6 MW
Power
0.3 MW
L&D
0.4 MW
Power
1.4 MW
Wheat straw
102.0 MW
(6.22 kg/s)
Hydrothermal pretreatment
Fibre fraction
71.2 MW
Liquefaction
Liquefied fibre fraction
68.0 MW
Liquid fraction
36.4 MW
Product flow
Heat flow
Power flow
Loss & destruction
SSF
CO2: ~0
MW
Recovered Heat
5.3 MW
L&D
4.0 MW
Power
1.5 MW
Heat
6.1 MW
Recovered Heat
0.8 MW
L&D
1.0 MW
Power
0.1 MW
Heat
2.3 MW
Separation
Fibre stillage
42.4 MW
Distillation
Fermentation broth
68.0 MW
L&D
4.4 MW
Solid biofuel
49.5 MW
Molasses
27.6 MW
Ethanol
26.2 MW

Figure 4 - caption

Figure 4 – Grassmann diagram illustrating exergy flows in the ethanol facility. Exergy losses and destruction (L&D) for the individual components are also indicated.

Figure 5

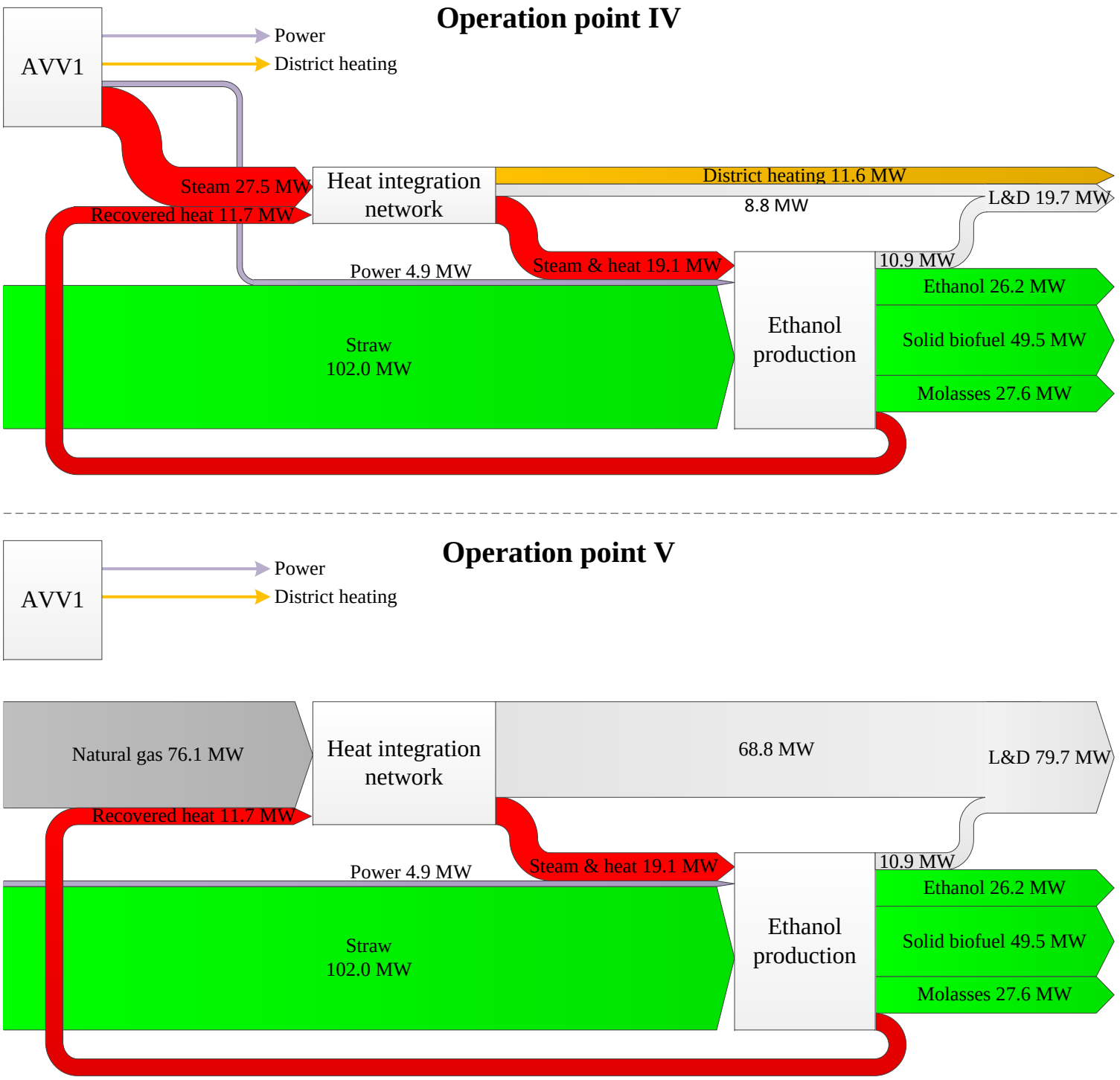
Operation point IV
AVV1
Power
District heating
Steam 27.5 MW
Recovered heat 11.7 MW
Heat integration network
District heating 11.6 MW
8.8 MW
L&D 19.7 MW
Steam & heat 19.1 MW
10.9 MW
Power 4.9 MW
Straw
102.0 MW
Ethanol production
Ethanol 26.2 MW
Solid biofuel 49.5 MW
Molasses 27.6 MW
Operation point V
AVV1
Power
District heating
Natural gas 76.1 MW
Recovered heat 11.7 MW
Heat integration network
68.8 MW
L&D 79.7 MW
Steam & heat 19.1 MW
10.9 MW
Power 4.9 MW
Straw
102.0 MW
Ethanol production
Ethanol 26.2 MW
Solid biofuel 49.5 MW
Molasses 27.6 MW

Figure 5 - caption

Figure 5 – Grassmann diagrams of the integrated process in operation points IV (top) and V (bottom).